7-Aminoactinomycin Binding to DNA Sequences Lacking GpC Sites: A Thermodynamic and Kinetic Study

Tarita Biver,[‡] Marcella Venturini,[‡] Elizabeth A. Jares-Erijman,[§] Thomas M. Jovin,[||] and Fernando Secco*[,‡]

Dipartimento di Chimica e Chimica Industriale, Università di Pisa, Via Risorgimento 35, 56126 Pisa, Italy, Departamento de Química Orgánica, Facultad de Ciencias Exactas y Naturales, Universidad de Buenos Aires, Ciudad Universitaria Pabellón II/3, 1428 Buenos Aires, Argentina, and Laboratory of Cellular Dynamics, Max Planck Institute for Biophysical Chemistry, am Fassberg 11, 37077 Göttingen, Germany

Received September 3, 2008; Revised Manuscript Received November 6, 2008

ABSTRACT: The interaction of 7-aminoactinomycin (7AAMD) with selected DNA sequences (TAGTTA, R5, HP5, and HP1) of different lengths and secondary structures, all containing a 5′-TAGT-3′ block, was studied at an ionic strength of 0.02 M and pH 7.7 by means of fluorescence equilibrium and kinetic (stopped-flow) measurements. Both approaches indicated that the antibiotic binds strongly to both the single-stranded and hairpin (HP1) structures, although the sequences lacked the canonical GpC sites favored by actinomycin. Binding isotherms and initial rate analyses revealed that the binding stoichiometry was 1:1 in all cases. While the single-stranded sequences displayed a simple monoexponential kinetic behavior, the binding of 7AAMD to HP1 at <30 °C was biphasic and could be rationalized in terms of a sequential formation of two isomeric bound forms or alternatively in terms of an ssHP1−hpHP1 equilibrium, with both HP1 forms reacting with 7AAMD. The rates of complex dissociation induced by the detergent SDS were also measured. After correction of the kinetic traces for spurious effects that can be attributed to the SDS, monoexponential traces were obtained, with relaxation times in agreement with the kinetics of complex formation.

Actinomycin D (AMD)[1] is a widely studied drug, and widespread interest in it stems from its function as an antitumor agent and as a model sequence-specific antibiotic (*1*−*3*). It has been established that the drug binds to DNA by intercalation (*4*), showing a preference for dG-dC sequences (*1*, *5*). However, strong binding to polynucleotides devoid of GpC sites was also found to occur (*6*, *7*). Moreover, the importance of the site-flanking residues has also been established (*8*−*10*). It has been previously reported that AMD and its fluorescent 7-amino analogue (7AAMD) are able to bind with high affinity to particular single-stranded DNA (ssDNA) sequences (*6*, *11*−*14*) and that such interactions may be involved in the inhibition by AMD of HIV reverse transcriptase and other enzymes requiring ssDNA. Further elucidation of the features of interaction of AMD with the different secondary structures of DNA is thus of great importance for improving our understanding of the biological activity of this drug and for developing new antitumor/antiviral agents with improved target selectivity.

Significant progress has been made in the elucidation of the structural features of actinomycin−DNA complexes (*15*−*18*), but the mechanism of the binding process remains poorly understood probably because of its complexity. A pioneering kinetic study by Müller and Crothers (*1*) on complexes of AMD with calf thymus DNA revealed the occurrence of at least five separate processes, of which only two (the fastest) were concentration-dependent. The authors proposed that several conformational states, differing in the positions of the peptide rings, arise in sequence with an evolution of the most rapidly forming species toward stable structures. The results of Müller and Crothers were confirmed subsequently (*19*) in investigations of defined synthetic DNAs. Fox and Waring (*20*) proposed a different model according to which the antibiotic initially binds to many sequences on a heterogeneous DNA lattice and then "shuffles" between the available sites until a thermodynamically determined optimum state of binding is attained. More recently, Chen and Jones (*21*) found that the kinetics of dissociation of AMD from oligonucleotides with hairpin motifs display two rate constants that were associated with hairpin and duplex conformations present at equilibrium. Further work of Chen (*9*) on dissociation of AMD from DNA with CXG repeats provided a satisfactory monoexponential description of the kinetic behavior.

We present here a thermodynamic and kinetic study of the interaction of the fluorescent AMD derivative, 7AAMD, with selected DNA sequences of different lengths and secondary structures.

* To whom correspondence should be addressed. E-mail: ferdi@dcci.unipi.it. Telephone: +39-050-2219259. Fax: +39-050-2219260.
[‡] Università di Pisa.
[§] Universidad de Buenos Aires.
[||] Max Planck Institute for Biophysical Chemistry.

[1] Abbreviations: AMD, actinomycin D; 7AAMD, 7-aminoactinomycin D; TAGTTA, 5′-TAGTTA-3′; R5, 5′-AAAAAAAAAAT-AGTTTTAAATATTT-3′; HP5, 5′-TAGTTTTAAATA-3′; HP1, 5′-AAAAAAATAGTTTTAAATATTTTTTT-3′; SDS, sodium dodecyl sulfate; ssDNA, single-stranded DNA; ssHP1, single-stranded HP1; hpHP1, hairpin HP1.

10.1021/bi801671c CCC: $40.75
Published on Web 12/10/2008

TAGTTA	5'-	TAGTTA	-3'
R5	5'-	AAAAAAAAAATAGTTTTAAATATTT	-3'
HP5	5'-	TAGTTTTAAATA	-3'
HP1	5'-	AAAAAAATAGTTTTAAATATTTTTTT	-3'

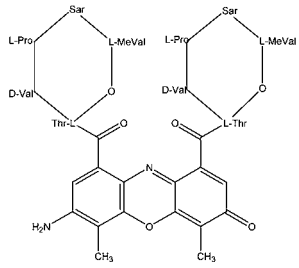

FIGURE 1: Oligonucleotide sequences used in this work and structure of 7-aminoactinomycin (7AAMD).

EXPERIMENTAL PROCEDURES

Materials. 7-Aminoactinomycin D (7AAMD) was purchased from Sigma and used without further purification. The concentrations of 7AAMD solutions in water were determined spectrophotometrically using a molar extinction coefficient (ε_D) of 21900 M^{-1} cm^{-1} at 505 nm (*22*). The synthetic oligonucleotides designated as R5, HP1, and HP5 (Figure 1) [the designations correspond to those employed in previous investigations performed on the same synthetic fragments (*10*, *13*)] and the hexamer TAGTTA were purchased from Metabion. The oligonucleotides were synthesized by standard solid-phase techniques and purified by high-performance liquid chromatography (HPLC). The oligonucleotide concentrations in strands were obtained spectrophotometrically with molar extinction values calculated for 260 nm according to the nearest-neighbor approximation using mono- and dinucleotide values tabulated by Fasman (*23*): ε_{R5} = 272300 M^{-1} cm^{-1}, ε_{HP1} = 268700 M^{-1} cm^{-1}, ε_{HP5} = 126600 M^{-1} cm^{-1}, and ε_{TAGTTA} = 64300 M^{-1} cm^{-1}. Sodium dodecyl sulfate (SDS) was the 99% ACS reagent (Aldrich). All measurements were taken in a buffer solution at pH 7.7 [10 mM sodium cacodylate, 10 mM NaCl, and 0.1 mM Na_2EDTA] and, unless stated otherwise, at 20 °C. Doubly distilled water was used to prepare all solutions.

Methods. (i) Thermodynamics. Absorbance measurements were performed with a Perkin-Elmer Lambda 35 spectrophotometer and fluorescence titrations with a Perkin-Elmer (Überlingen, Germany) LS55 spectrofluorometer with a λ_{exc} of 532 nm and a λ_{em} of 630 or 615 nm. The titrations were carried out by adding increasing amounts of the oligonucleotide directly to the cell containing the dye solution. Both instruments were equipped with jacketed cell holders maintaining temperature control within ±0.1 °C. Experimental data were analyzed by means of nonlinear least-squares fitting procedures performed by a Jandel (AISN software) program.

(ii) Kinetics. The kinetic experiments were performed at 20 °C on both an Applied Photophysics stopped-flow fluorometer and a stopped-flow apparatus assembled in our laboratory (Pisa) from a Hi-Tech SF-61 mixing unit connected to the spectrofluorimetric line by optical quartz fibers

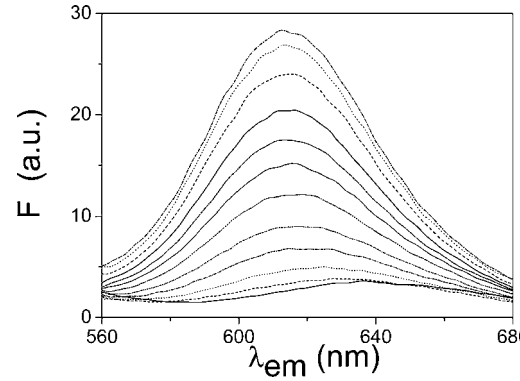

FIGURE 2: Fluorescence spectra recorded upon addition of increasing amounts of oligonucleotide R5 to the dye 7AAMD. $[D_{tot}]$ = 0.66 μM, pH 7.7, ionic strength of 0.02 M, 20 °C, λ_{exc} = 532 nm, λ_{em} = 630 nm. From bottom to top: $[P_{tot}]/[D_{tot}]$ = 0, 0.13, 0.38, 0.76, 1.3, 2.2, 3.2, 4.5, 6.4, 11, 19, and 25.

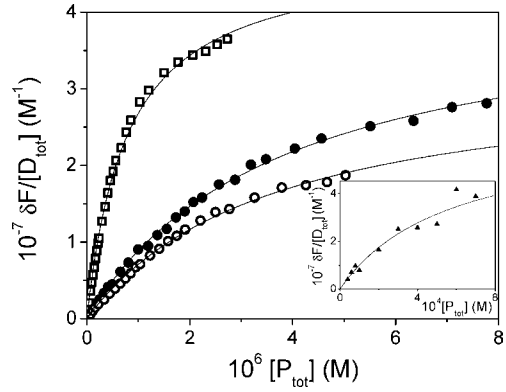

FIGURE 3: Binding isotherms from spectrofluorimetric titrations for different 7AAMD−oligonucleotide systems. Conditions as described in the legend of Figure 2: (●) 7AAMD−R5 where $[D_{tot}]$ = 0.66 μM, (○) 7AAMD−HP5 where $[D_{tot}]$ = 0.74 μM, and (□) 7AAMD−HP1 where $[D_{tot}]$ = 0.60 μM. The inset is relative to the 7AAMD−TAGTTA system where $[D_{tot}]$ = 9.9 μM.

(*24*). In the first case, excitation light was obtained from a xenon lamp (505 nm), whereas in the latter case, excitation was with a green laser diode (4 mW, 532 nm). The reaction transients were stored and transferred to a personal computer for analysis by means of least-squares fitting procedures using the Jandel program. Experiments aimed at complex dissociation were conducted by mixing a solution containing the completely formed 7AAMD−oligo complex with an equal volume of a solution containing 2% SDS. Each experiment was repeated at least 10 times. The observed spread of time constants and/or initial rates was within 10%, and the mean values are reported.

RESULTS

Thermodynamics. Addition of increasing amounts of oligonucleotide to a cell containing the antibiotic produced an increase in fluorescence emission intensity, together with a blue shift of the emission maximum for all 7AAMD−oligomer systems investigated here (Figure 2). The binding isotherms obtained from fluorescence measurements are shown in Figure 3 for the 7AAMD−R5, 7AAMD−HP1, and 7AAMD−HP5 systems. In the case of the 7AAMD−TAGTTA system, the binding experiments revealed a much lower affinity for the hexanucleotide (1−3 mM^{-1}), reflected in relatively large errors (inset of Figure 3) despite the addition of a large excess

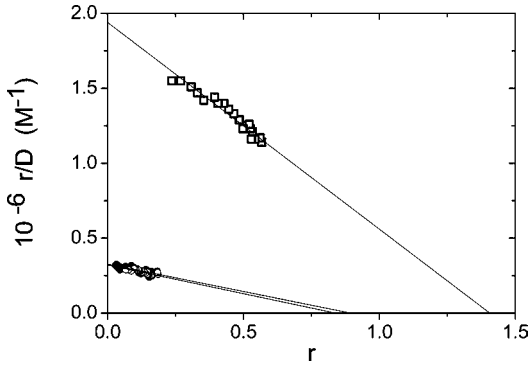

FIGURE 4: Scatchard plots of the spectrofluorimetric titrations. Conditions as described in the legend of Figure 2: (●) 7AAMD−R5, (○) 7AAMD−HP5, and (□) 7AAMD−HP1.

of DNA (up to 0.7 mM). The analysis of the titration data was carried out assuming the equilibrium

$$P + D \underset{k_f}{\overset{k_d}{\rightleftharpoons}} PD \quad (1)$$

where P is the free DNA, D the free dye, and PD the complex. Scatchard plots of the spectrofluorimetric titrations (Figure 4) provided initial estimates of binding constant K_a and site size n (Table 1). In contrast to previous reports (*25*), the value of n was found to be close to unity for all the investigated systems (Table 1). Thus, a data treatment according to a Benesi−Hildebrand (eq 2) plot was employed in evaluating the equilibrium constants

$$\frac{[D_{tot}]}{\delta F} = \frac{1}{\Delta F}\left(\frac{1}{K_a}\frac{1}{[P]} + 1\right) \quad (2)$$

where $[D_{tot}]$ is the total dye concentration, $\delta F = F - F^D$ is the fluorescence intensity variation, $\Delta F = F^{PD} - F^D$ (*26*), and [P] now represents the free strand concentration at equilibrium. The intercept/slope ratio of the straight line corresponding to the best fit to the experimental data yields the equilibrium constant. Inasmuch as the determination of [P] depends on K_a, an iterative procedure was employed, starting with the approximation $[P] = [P_{tot}]$. The results of such an analysis are shown in Figure 5, and the values of K_a for the 7AAMD−R5, 7AAMD−HP5, and 7AAMD−HP1 systems are collected in Table 1.

Kinetics of the 7AAMD−R5 and 7AAMD−HP5 Systems. The kinetics of the interaction of 7AAMD with R5 and HP5 were investigated under pseudo-first-order conditions ($[P_{tot}] > 10[D_{tot}]$). With the exception of the 7AAMD−R5 system, which at low temperatures ($T < 15$ °C) tends to form double strands (see a stopped-flow experiment at 12 °C in the Supporting Information), satisfactory monoexponential stopped-flow curves were obtained, as shown in Figure 6. The reciprocal relaxation times were found to change with reactant concentrations according to the linear relationship

$$1/\tau = k_f([P] + [D]) + k_d \quad (3)$$

where k_f and k_d are the rate constants for complex formation and dissociation, respectively, according to reaction 1. The evaluation of equilibrium concentrations [P] and [D] required knowledge of K_a. As a first approximation, the concentration variable ([P] + [D]) was replaced in eq 3 by the sum of the total concentrations of the reacting species ($[P_{tot}] + [D_{tot}]$). The equilibrium constant obtained from the resulting k_f and k_d values was used to re-evaluate [P] + [D] and replot the data. This procedure was repeated until convergence was achieved. Plots according to eq 3 for the 7AAMD−R5 and 7AAMD−HP5 systems are shown in Figure 7. A few experiments performed under reversed excess species conditions, i.e., $[D_{tot}] > 10[P_{tot}]$, yield results in agreement with the other determinations (stars in Figure 7).

These results show that the reaction was first-order both in [P] and [D]. Several experiments under non-pseudo-first-order conditions were also performed. Under these circumstances, eq 4, which can be applied to any second-order reaction, has been used to analyze the kinetic data.

$$[PD] = \frac{f(e^{-wk_f t} - 1)}{(xe^{-wk_f t} - y)} \quad (4)$$

where $f = 2[D_{tot}][P_{tot}]$, $w = (z^2 - 2f)^{1/2}$, $z = [D_{tot}] + [P_{tot}] + (1/K_a)$, $x = z - w$, and $y = z + w$. K_a is kept at the fixed value obtained by spectrofluorometric titrations. Equation 4 has been obtained from the integrated rate equation applicable to reaction 1 under conditions where $[P_{tot}] \neq [D_{tot}]$ (*27*). As [PD] is proportional to the signal change, a fit of the kinetic traces according to eq 4 provides the value of k_f. The values of k_f and k_d ($=k_f/K_a$) so obtained are reported in Table 1.

Formation of the 7AAMD−HP1 Complex. Stopped-flow experiments on the binding of the 7AAMD−HP1 system, performed at 20 °C, reveal the occurrence of a biphasic process. Curve fitting according to the second-order equation valid for cases in which $[P_{tot}] \neq [D_{tot}]$ (eq 4) displayed distinct deviations from experiment (Figure 8A). The kinetic behavior at 20 °C could be rationalized assuming the series mechanism represented by eq 5

$$P + D \underset{k_1}{\overset{k_{-1}}{\rightleftharpoons}} PD_1 \underset{k_2}{\overset{k_{-2}}{\rightleftharpoons}} PD_2 \quad (5)$$

HP1 at 20 °C is present mainly in the hairpin configuration. In the first step, complex PD_1 forms which, in the second step, evolves to the more stable form, PD_2. Increasing the D (and under some conditions P) concentration in such a way that pseudo-first-order conditions are fulfilled leads to monophasic reactions. This behavior could be rationalized assuming that under these circumstances, the first step undergoes equilibration so rapidly that its rate becomes too high to be measured by the stopped-flow method, so that the second of the two steps is rate-determining. The rate equation for reaction 5 then becomes

$$1/\tau = K_1 k_2([P] + [D])/[1 + K_1([P] + [D])] + k_{-2} \quad (6)$$

where $K_1 = k_1/k_{-1}$.

The observed linear trend (Figure 7) of the $1/\tau$ versus [P] + [D] plot indicates that $K_1 < 10^3$ M^{-1}, since otherwise a downward bending of the data points would have been observed for the highest values of [P] + [D]. The values of the rate constants obtained are reported in Table 1.

Experiments performed at 40 °C, where HP1 is single-stranded (*25*), exhibited a monoexponential behavior (Figure 8B). The data obtained under non-pseudo-first-order conditions were nicely fitted by a second-order equation valid for cases in which $[P_{tot}] \neq [D_{tot}]$ (eq 4). A plausible mechanism involves the direct binding of D to single strands of HP1 according to eq 1.

Table 1: Kinetic and Equilibrium Parameters for the 7AAMD−HP1, 7AAMD−R5, 7AAMD−HP5, and 7AAMD−TAGTTA Systems at 20 °C and pH 7.7 with an Ionic Strength of 0.02 M

oligonucleotide	k_f ($\times 10^{-6}$ M^{-1} s^{-1})	k_d (s^{-1})	K_a[a] ($\times 10^{-5}$ M^{-1})	K_a[b] ($\times 10^{-5}$ M^{-1})	K_a[c] ($\times 10^{-5}$ M^{-1})	n[c]
TAGTTA				0.02 ± 0.01		
R5	7.1 ± 0.9	37.4 ± 0.5	1.9 ± 0.5	2.9 ± 0.5	3.3 ± 0.2	1.0 ± 0.2
	9.7 ± 1.5[d]	33.5 ± 5.2[e]				
HP5	7.5 ± 0.6	15.2 ± 3.2	4.8 ± 1.4	4.0 ± 0.6	3.2 ± 0.2	1.2 ± 0.2
	9.7 ± 1.7[d]	24.3 ± 4.2[e]				
HP1	0.76 ± 0.04	0.42 ± 0.24	18 ± 9	16 ± 1	19 ± 2	0.71 ± 0.15
	0.89 ± 0.20[d]	0.56 ± 0.13[e]				
		0.20 ± 0.02[f]				

[a] Kinetics equation (*3*). [b] Thermodynamics equation (*2*). [c] Scatchard plots. [d] Kinetics equation (*4*). [e] $k_d = k_f/K_a$. [f] Detergent-induced dissociation.

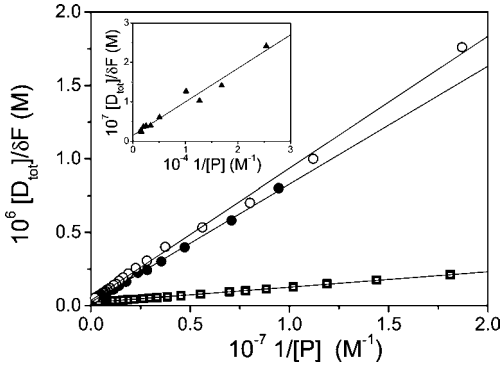

FIGURE 5: Analysis of the spectrofluorimetric titrations based on eq 2. Conditions as described in the legend of Figure 2: (●) 7AAMD−R5, (○) 7AAMD−HP5, and (□) 7AAMD−HP1. The inset is for 7AAMD−TAGTTA.

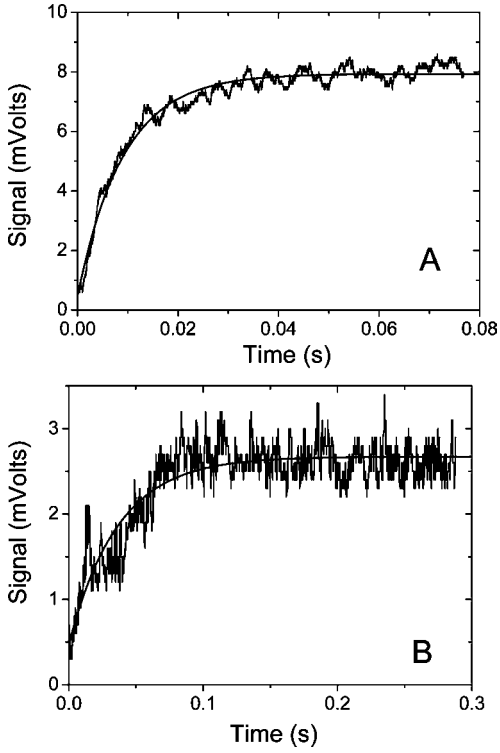

FIGURE 6: Stopped-flow kinetic curves for the 7AAMD−R5 and 7AAMD−HP5 systems. Conditions as described in the legend of Figure 2. (A) 7AAMD−R5: $[P_{tot}] = 4.3$ μM, $[D_{tot}] = 0.33$ μM, and $\tau = 9.2$ ms. (B) 7AAMD−HP5: $[P_{tot}] = 4.1$ μM, $[D_{tot}] = 0.31$ μM, and $\tau = 36.5$ ms. The solid lines are the monoexponential fits.

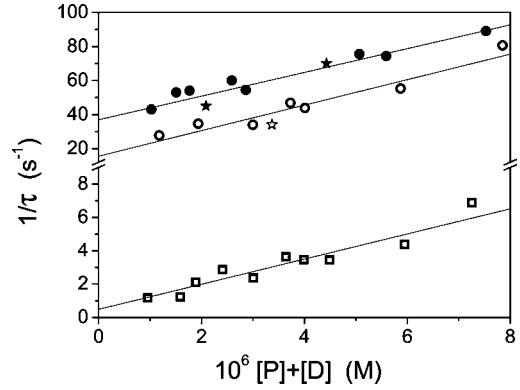

FIGURE 7: Reciprocal relaxation time vs reactant concentration at pH 7.7, an ionic strength of 0.02 M, and 20 °C: (●) 7AAMD−R5, (○) 7AAMD−HP5, and (□) 7AAMD−HP1. The straight lines interpolating data points are drawn following eq 3, and stars refer to particular experimental conditions described in the text.

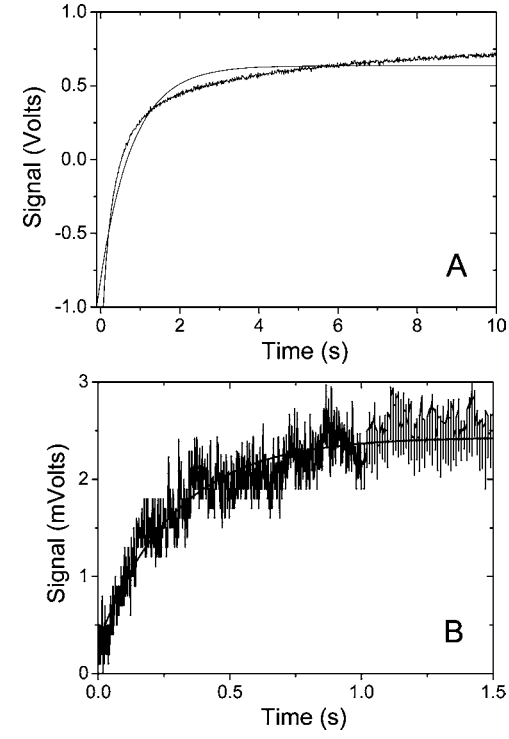

FIGURE 8: Stopped-flow kinetic curves for the 7AAMD−HP1 system at pH 7.7 and an ionic strength of 0.02 M. (A) $T = 20$ °C, $[P_{tot}] = 4.0$ μM, and $[D_{tot}] = 2.0$ μM. (B) $T = 40$ °C, $[P_{tot}] = 0.06$ μM, $[D_{tot}] = 4.5$ μM, and $\tau = 290$ ms. The solid lines are the fits according to eq 4.

Initial Rates of Complex Formation. The complex formation reactions of 7AAMD with R5 and HP1 were also investigated under nearly second-order conditions. The values of the initial rates (V_0, expressed as Δsignal/Δtime) of complex formation were derived from straight line interpolations of the initial segments of the kinetic curves. The dye

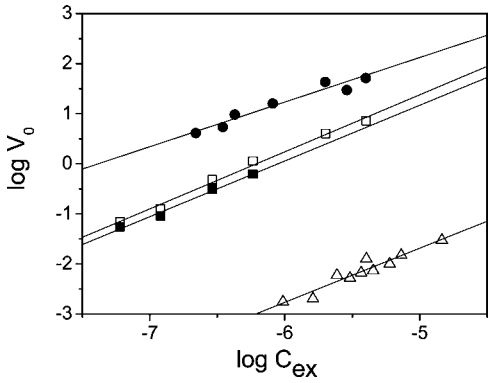

FIGURE 9: Dependence of the initial rate on reagent concentration. Conditions as described in the legend of Figure 2. (●) 7AAMD−R5: $C_{ex} = [P_{tot}]$, $[D_{tot}] = 2.0$ μM, and 20 °C. (□) 7AAMD−HP1: $C_{ex} = [P_{tot}]$, $[D_{tot}] = 2.0$ μM, and 20 °C. (■) 7AAMD−HP1: $C_{ex} = [P_{tot}]$, $[D_{tot}] = 2.0$ μM, and 40 °C. (△) 7AAMD−HP1: $C_{ex} = [D_{tot}]$, $[P_{tot}] = 0.06$ μM, and 20 °C. The slope of the logarithmical plots is the reaction order with respect to the excess reagent that turned out to be equal to 1 in all cases.

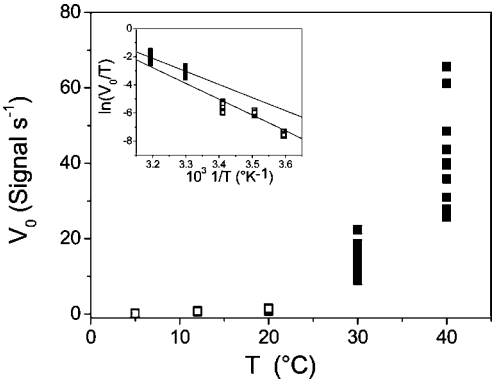

FIGURE 10: Dependence of the initial rate on temperature for the 7AAMD−HP1 system at pH 7.7 with an ionic strength of 0.02 M where $[P_{tot}] = 0.25$ μM and $[D_{tot}] = 2.0$ μM: (□) before secondary structure melting and (■) after melting. The inset shows the Eyring plots whose slopes yield the activation enthalpy variation.

concentration was kept constant at 2 μM, and the oligonucleotide concentration was varied in the range of 0.22−4 μM for the 7AAMD−R5 system and in the range of 0.12−4 μM for the 7AAMD−HP1 system. Plots of log V_0 versus log C_{ex} enabled a determination of the reaction order with respect to the oligonucleotide; a value of unity was obtained for both R5 and HP1 at 20 °C [Figure 9 (● and □)]. Two experiments were also performed at 40 °C where HP1 would be single-stranded. The reaction order was again 1 [Figure 9 (■)]. The same result was obtained under a constant oligomer concentration (0.06 μM) and at a dye concentration in the range of 1−15 μM [Figure 9 (△)].

The dependence of the initial rate on temperature for the 7AAMD−HP1 system was also investigated. The plot of V_0 versus T was biphasic, with a sudden increase in the rates above the melting temperature (Figure 10). Eyring plots (inset of Figure 10) led to estimates of the activation enthalpy ($\Delta H^{\ddagger}$) for measurements conducted below and above the melting point (T_m): $\Delta H^{\ddagger} = 92$ kJ/mol ($T < T_m$), and $\Delta H^{\ddagger} = 75$ kJ/mol ($T > T_m$).

The effect on the reaction rate produced by changes in salt concentration in the ionic strength range of 0.0002−0.02 M was negligible (data not shown), as would be expected for the binding of a neutral molecule such as 7AAMD.

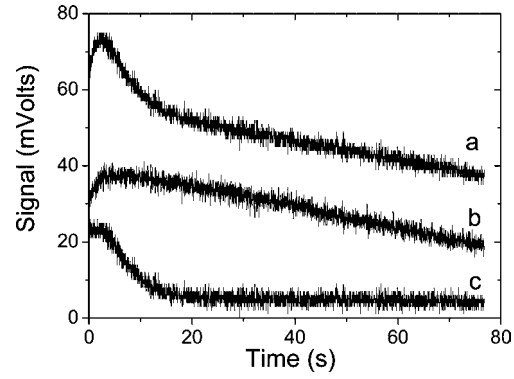

FIGURE 11: Stopped-flow kinetic curves for detergent-induced dissociation of the 7AAMD−HP1 complex. Conditions as described in the legend of Figure 2. (a) 7AAMD−HP1 complex added to SDS: $[P_{tot}] = 0.41$ μM, $[D_{tot}] = 0.41$ μM, and [SDS] = 0.035 M. (b) Blank test 7AAMD only added to SDS: $[D_{tot}] = 4.0$ μM and [SDS] = 0.035 M. (c) Experimental curve a corrected for blank effects b.

Complex Dissociation. Detergent-induced dissociation experiments of the 7AAMD−HP1 complex were also performed. A kinetic curve, recorded after the mixing of preformed 7AAMD−HP1 complex with SDS, is shown in Figure 11a. Three different effects were observed, while control experiments, in which only 7AAMD was reacted with SDS, displayed two kinetic effects (Figure 11b) whose parameters ($\alpha_1 = 11.8$ mV, and $\tau_1 = 0.72$ s; $\alpha_2 = 368$ mV, and $\tau_2 = 1546$ s) corresponded to the faster and slower of the three effects observed with the 7AAMD−HP1/SDS mixture. Thus, difference curves were generated, yielding a kinetic curve attributed only to the dissociation of the 7AAMD−HP1 complex (Figure 11c). The time course of this process was monoexponential [$1/\tau = 0.20 \pm 0.02$ s^{-1} ($\tau = 5$ s)].

DISCUSSION

As outlined in the introductory section, actinomycin D exhibits a high affinity for the 5′-TAGT-3′ block present in ssDNAs. This sequence motif was present in all the oligonucleotides investigated in this study, but while in TAGTTA, R5, and HP5 it is part of an unstructured region, as shown by the melting experiments, in HP1 below 30 °C, the adenine of the TAGT block is base paired with a thymine of the same strand because of the formation of a hairpin loop (*12*).

Short oligonucleotides with which interactions of the actinomycin peptide rings would have to be minimal were found to display little affinity for the drug, whereas longer sequences giving rise to secondary structures favored intercalation (*28*−*30*). TAGTTA is the shortest of the investigated sequences and would be expected to bind 7AAMD more weakly. However, its association equilibrium constant, although much lower compared to those of the other ssDNAs, was sufficiently high (2×10^3 M^{-1}) that it revealed the remarkable affinity of actinomycin for the TAGT block.

R5 and HP5 exhibited similar behavior. The rate constants for dye binding were similar, as were the rate constants for dye dissociation, in spite of the different lengths of the two DNAs. This observation indicates that the long A sequence preceding the TAGT block in R5 does not influence the rate parameters and (as a consequence) the equilibrium parameters. On the other hand, the sequences following TAGT

block in R5 and HP5 are rather similar and can interact with the peptide residues of 7AAMD with similar affinity (Table 1). In contrast, TAGTTA lacks such flanking sequences and thus displays a reduced affinity for the drug. The kinetics was strictly first-order for both DNA and the drug, thus showing that no equilibria between single strand and duplex were present in the investigated range of DNA concentrations. Strong evidence in support of this conclusion was provided in the case of the 7AAMD−R5 system by electrophoretic comigration of 7AAMD with the relevant complex (*14*).

The reaction constants for 7AAMD binding to R5 and HP5 were distinctly lower than the corresponding parameters measured for simple drug binding to single strands. Hemi-intercalation of proflavine into ss-poly(A) occurs in a few microseconds (*31*), and even intercalation into DNAs of simple dyes is faster compared to that in the systems here discussed. The dramatic reduction in rate reveals the important role played by the peptide rings flanking the central intercalating residue. These peptide moieties in principle can bind very quickly to DNA and thereby create an energy barrier to optimal positioning of the planar residue between A and G bases of the TAGT block. The agreement between the equilibrium constants evaluated from thermodynamics and, independently, from kinetics confirms that the observed first-order behavior represents a simple binding process. The nonmonoexponential kinetic traces found for the 7AAMD−R5 system at <15 °C can be explained taking into account the fact that at lower temperatures a single strand−double strand equilibrium is established (*25*), which is necessarily coupled to the binding step.

The melting profile of HP1 indicates this DNA is single-stranded at >30 °C and double-stranded below that temperature. The structure of HP1 is such that the probability of forming a hairpin is much higher than that of associating to form a duplex. Actually, the 7AAMD−HP1 system displays an association equilibrium constant almost 1 order of magnitude higher than that for the 7AAMD−R5 and 7AAMD−HP5 systems and 3 orders of magnitude higher than for the 7AAMD−TAGTTA system. These large differences strongly suggest an interaction process more similar to intercalation than to hemi-intercalation.

The experiments at 40 °C showed that 7AAMD bound to single-stranded HP1 as well. Hence, the reaction mechanism shown in scheme 7 could be taken into account as well, as an alternative to scheme 5, which is justified by the observation from the equilibrium studies that a single final product (PD) is obtained.

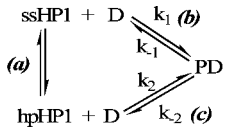

(7)

Note that the bound HP1 is in the hairpin configuration; hence, step b should involve dye binding to single-stranded DNA to form PD, whereas the bound ssHP1 winds so that PD presents a hairpin configuration (*25*). Reaction scheme 7, containing two thermodynamically independent steps, in principle gives rise to a biphasic behavior. One can assume that the ssHP1 ⇆ hpHP1 interconversion (step a) is fast and that dye binding to and dissociation of dye from ssHP1 (step b) is faster than step c, which is reasonable since interaction of the dye with single strands is faster than interaction with double strands. Under these circumstances, an increase in [D] allows step b to be considered as a pre-equilibrium so that such a reaction becomes monophasic. Note that a stopped-flow measurement of binding of 7AAMD to HP1 with $[P_{tot}]/[D_{tot}] = 5$ displays monoexponential features (*32*).

With respect to kinetic studies of detergent-induced dissociation, we stress the importance of suitable control reactions for discriminating between the inherent drug−DNA dissociation and other detergent-related processes. To clarify the nature of the two spurious effects observed with HP1, experiments involving mixing SDS alone with buffer were also performed. The slower but not the faster effect was evident. As it is known that at relatively high concentration SDS micelles are able to adopt conformations other than spherical, the slowest of the observed effects (min time range) may be related to a slow conformational change of the SDS micelles after dilution in the stopped-flow apparatus. The fastest spurious effect was observed upon mixing 7AAMD with SDS, whereas the intermediate process was attributable to dissociation of the 7AAMD−HP1 complex. The value of the dissociation rate constant (0.2 s^{-1}) was in agreement with the value of 0.4 ± 0.2 s^{-1} obtained from the kinetics of complex formation.

The activation enthalpy values obtained for the 7AAMD−HP1 complex have a large uncertainty due to the restricted experimentally accessible temperature range, but yet agreed with those reported for similar oligonucleotide systems (*33*), even though higher values (150−200 kJ/mol) have been suggested for strongly coupled and closed hairpins (*21*). The lower activation energy value found after HP1 melting can be rationalized by assuming an increased accessibility of the drug to the open sites of single-stranded HP1.

CONCLUSIONS

Equilibrium titrations show that 7AAMD binds to R5, HP1, and HP5 oligonucleotides, forming stable complexes with 1:1 stoichiometry. The binding to the shorter TAGTTA hexamer is much weaker. Stopped-flow kinetics of complex formation and dissociation confirm the thermodynamic results, both methods suggesting that while R5 and HP5 react with the dye in their single-strand conformation, HP1 reacts in the form of a hairpin at <30 °C and as a single strand at higher temperatures.

ACKNOWLEDGMENT

T.B. gratefully acknowledges the Laboratory of Cellular Dynamics of the Max Planck Institute for Biophysical Chemistry for instrument facilities.

SUPPORTING INFORMATION AVAILABLE

Stopped-flow kinetic curve for the 7AAMD/R5 system at 12 °C. This material is available free of charge via the Internet at http://pubs.acs.org.

REFERENCES

1. Müller, W., and Crothers, D. M. (1968) Binding of actinomycin and related compounds to DNA. *J. Mol. Biol. 35*, 251–290.
2. Waring, M. J. (1981) DNA modification and cancer. *Annu. Rev. Biochem. 50*, 159–162.

3. Goldberg, I. H., Beerman, T. A., and Poon, R. (1977) in *Cancer 5: A Comprehensive Treatise* (Becker, F. F., Ed.) pp 427−456, Plenum, New York.
4. Waring, M. J. (1970) Variation of the supercoils in closed circular DNA by binding of antibiotics and drugs. Evidence for molecular models involving intercalation. *J. Mol. Biol. 54*, 247–279.
5. Kamitori, S., and Takusasawa, F. (1992) Crystal structure of the 2:1 complex between d(GAAGCTTC) and the anticancer drug actinomycin D. *J. Mol. Biol. 225*, 445–456.
6. Wadkins, R. M., and Jovin, T. M. (1991) Actinomycin D and 7-aminoactinomycin D binding to single-stranded DNA. *Biochemistry 30*, 9469–9478.
7. Chen, F. M., and Sha, F. (2001) Actinomycin D binds strongly to d(TGTCATTG), a single-stranded DNA devoid of GpC sites. *Biochemistry 40*, 5218–5225.
8. Goodisman, J., Rehfuss, R., Ward, B., and Dabrowiak, J. C. (1992) Site-specific binding constants for actinomycin D on DNA determined from footprinting studies. *Biochemistry 31*, 1046–1058.
9. Chen, F. M. (1998) Binding of actinomycin D to DNA oligomers of CXG trinucleotide repeats. *Biochemistry 37*, 3955–3964.
10. Shafer, R. H., Burnette, R. R., and Mirau, P. A. (1980) Spectroscopic analysis of the equilibrium and kinetic DNA binding properties of several actinomycin analogues. *Nucleic Acids Res. 8*, 1121–1132.
11. Yoo, H., and Rill, R. L. (2001) Actinomycin D binding to unstructured, single-stranded DNA. *J. Mol. Recognit. 14*, 145–150.
12. Wadkins, R. M., Tung, C. S., Vallone, P. M., and Benight, A. S. (2000) The role of the loop in binding of an actinomycin D analog to hairpins formed by single-stranded DNA. *Arch. Biochem. Biophys. 384*, 199–203.
13. Jares-Erijman, E. A., Klement, R., Machinek, R., Wadkins, R. M., Kankia, B. I., Marky, L. A., and Jovin, T. M. (1997) Binding of actinomycin D to single-stranded DNA. *Nucleosides Nucleotides 16*, 661–667.
14. Wadkins, R. M., Jares-Erijman, E. A., Klement, R., Rüdiger, A., and Jovin, T. M. (1996) Actinomycin D binding to single-stranded DNA: sequence specificity and hemi-intercalation model from fluorescence and ^{1}H NMR spectroscopy. *J. Mol. Biol. 262*, 53–68.
15. Alexopoulos, E., Jares-Erijman, E. A., Jovin, T. M., Klement, R., Machinek, R., Sheldrick, G. M., and Uson, I. (2005) Crystal and solution structures of 7-amino-actinomycin D complexes with d(TTAGBrUT), d(TTAGTT) and d(TTTAGTTT). *Acta Crystallogr. D61*, 407–415.
16. Hou, M. H., Robinson, H., Gao, Y. G., and Wang, A. H.-J. (2002) Crystal structure of actinomycin D bound to the CTG triplet repeat sequences linked to neurological diseases. *Nucleic Acids Res. 30*, 4910–4917.
17. Robinson, H., Gao, Y. G., Yang, X., Sanishvili, R., Joachimiak, A., and Wang, A. H.-J. (2001) Crystallographic analysis of a novel complex of actinomycin D bound to the DNA decamer CGATCGATCG. *Biochemistry 40*, 5587–5592.
18. Takusagawa, H. L., and Takusagawa, F. (2000) Crystallization and preliminary X-ray diffraction studies of d(ACGTAGCTACGT)$_2$:[actinomycin D, (echinomycin)$_2$] and d(ACGTAGCTACGT)$_2$:[actinomycin D, (triostin A)$_2$] complexes. *Acta Crystallogr. D56*, 344–347.
19. Bittman, R., and Blau, L. (1975) Stopped-flow kinetic studies of actinomycin binding to DNAs. *Biochemistry 14*, 2138–2145.
20. Fox, K. R., and Waring, M. J. (1984) Kinetic evidence for redistribution of actinomycin molecules between potential DNA-binding sites. *Eur. J. Biochem. 145*, 579–586.
21. Chen, F. M., Jones, C. M., and Johnson, Q. L. (1993) Dissociation kinetics of actinomycin D from oligonucleotides with hairpin motifs. *Biochemistry 32*, 5554–5559.
22. Sengupta, S. K., and Shaer, D. (1978) The interaction of 7-substituted actinomycin D analogs with DNA. *Biochim. Biophys. Acta 521*, 89–100.
23. Fasman, G. D., Ed. (1975) *CRC Handbook of Biochemistry and Molecular Biology*, 3rd ed., Vol. I, p 589, Chemical Rubber Publishing Co., Cleveland, OH.
24. D'Amico, M. L., Paiotta, V., Secco, F., and Venturini, M. (2002) A Kinetic Study of the Intercalation of Ethidium Bromide into Poly(A)Poly(U). *J. Phys. Chem. B 106*, 12635–12641.
25. Wadkins, R. M., Vladu, B., and Tung, C. S. (1998) Actinomycin D binds to metastable hairpins in single-stranded DNA. *Biochemistry 37*, 11915–11923.
26. Biver, T., Secco, F., and Venturini, M. (2005) Relaxation kinetics of the interaction between RNA and metal-intercalators: The Poly(A)Poly(U)/platinum-proflavine system. *Arch. Biochem. Biophys. 437*, 215–223.
27. Eq 4 has been derived by the authors.
28. Qu, X., Ren, J., Riccelli, P. V., Benight, A. S., and Chaires, J. B. (2003) Enthalpy/Entropy Compensation: Influence of DNA Flanking Sequence on the Binding of 7-Amino Actinomycin D to Its Primary Binding Site in Short DNA Duplexes. *Biochemistry 42*, 11960–11967.
29. Chen, F. M., Sha, F., Chin, K. H., and Chou, S. H. (2003) Unique actinomycin D binding to self-complementary d(CXYGGCCY'X'G) sequences: Duplex disruption and binding to a nominally base-paired hairpin. *Nucleic Acids Res. 31*, 4238–4246.
30. Chen, F. M., Sha, F., Chin, K. H., and Chou, S. H. (2003) Binding of Actinomycin D to Single-Stranded DNA of Sequence Motifs d(TGTCTnG) and d(TGTnGTCT). *Biophys. J. 84*, 432–439.
31. Ciatto, C., D'Amico, M. L., Natile, G., Secco, F., and Venturini, M. (1999) Intercalation of Proflavine and a Platinum Derivative of Proflavine into Double Helical Poly(A). *Biophys. J. 77*, 2717–2724.
32. Wershin, N., and Kovalev, A. (2006) Prompt non-stacking binding of actinomycin D to hairpin oligonucleotide HP1 and slow redistribution form HP1 to DNA. *J. Biochem. 140*, 185–191.
33. Brown, S. C., and Shafer, R. H. (1987) Kinetic studies of actinomycin D binding to mono-, oligo-, and polynucleotides. *Biochemistry 26*, 277–282.

BI801671C